Heliyon 9 (2023) e22083

Contents lists available at ScienceDirect

Heliyon

journal homepage: www.cell.com/heliyon

Integrating bulk and single-cell RNA sequencing data to establish necroptosis-related lncRNA risk model and analyze the immune microenvironment in hepatocellular carcinoma

Rongjie Zhang [a,1], Qian Li [a,1], Xiaoxiao Yu [a], Yiwen Hou [a], Liang Yan [d], Yating Gao [a], Longshan Ji [a], Xin Zhang [a], Miao Fang [a], Lingying Huang [c], Zhuo Yu [c], Yueqiu Gao [a,b,**], Man Li [a,*]

[a] Laboratory of cellular Immunity, Shuguang Hospital, Affiliated to Shanghai University of Traditional Chinese Medicine, China
[b] Institute of Infectious Diseases of Integrated Traditional Chinese and Western Medicine, China
[c] Department of Hepatopathy, Shuguang Hospital, Affiliated to Shanghai University of Traditional Chinese Medicine, China
[d] General Surgery Department of Shuguang Hospital Affiliated to Shanghai University of Traditional Chinese Medicine, China

ARTICLE INFO

Keywords:
Hepatocellular carcinoma
lncRNA
Necroptosis
Prognosis

ABSTRACT

Background: The increasing evidence suggests that necroptosis mediates many behaviors of tumors, as well as the regulation of the tumor microenvironment. Long non-coding RNAs (lncRNAs) are involved in a variety of regulatory processes during tumor development and are significantly associated with patient prognosis. It suggests that necroptosis-related lncRNAs (NRlncRNAs) may serve as biomarkers for the prognosis of hepatocellular carcinoma (HCC).

Methods: lncRNA expression profiles of HCC were obtained from TCGA database. LncRNAs associated with necroptosis were extracted using correlation analysis. Prognostic models were constructed based on least absolute shrinkage and selection operator algorithm (LASSO) and multivariate Cox regression analysis. The differences of tumor microenvironment between high-risk and low-risk groups were further analyzed. Single-cell RNA sequencing data of HCC was performed to assess the enrichment of necroptosis-related genes in immune cell subsets. Finally, real-time RT-PCR was used to detect the prognosis-related lncRNAs expression in different HCC cell lines.

Results: We constructed a prognostic signature based on 8 NRlncRNAs, which also showed good predictive accuracy. The model showed that the prognosis of patients with high-risk score was significantly worse than that of patients with low-risk score ($P < 0.05$). Combined with the clinical characteristics and risk score of HCC, Nomogram was drawn for reference in clinical practice. In addition, immune cell infiltration analysis and single cell RNA sequencing analysis showed that a low level of immune infiltration was observed in patients at high risk and that there was a significant correlation between NRlncRNAs and macrophages. The results of RT-qPCR also showed that 8 necroptosis-related lncRNAs were highly expressed in HCC cell lines and human liver cancer tissues.

* Corresponding author.
** Corresponding author. Laboratory of Cellular Immunity, Shuguang Hospital, Affiliated to Shanghai University of Traditional Chinese Medicine, China.
E-mail addresses: gaoyueqiu@shutcm.edu.cn (Y. Gao), liman121000@shutcm.edu.cn (M. Li).
[1] These authors made equal contributions to this work.

https://doi.org/10.1016/j.heliyon.2023.e22083
Received 25 April 2023; Received in revised form 1 November 2023; Accepted 3 November 2023
Available online 9 November 2023

Conclusion: This prognostic signature based on the necroptosis-related lncRNAs may provide meaningful clinical insights for the prognosis and immunotherapy responses in patients with HCC.

1. Introduction

As one of the most common malignant tumors, primary liver cancer ranks third among fatal cancers in China [1], with the most common type of the primary liver cancer being hepatocellular carcinoma (HCC) [2]. A variety of factors contribute to HCC, including hepatitis B virus (HBV), fatty liver, aflatoxin B1, hepatitis C virus (HCV), obesity, diabetes, iron overload, and cirrhosis caused by alcohol [3,4]. Among them, HBV, HCV infection and alcohol abuse are the most important causes of HCC worldwide [5,6]. With the popularization of HBV vaccination and the widespread use of antiviral drugs, the etiological pattern of HCC may be changing. In addition, the increase in nonalcoholic fatty liver disease (NAFLD), coupled with metabolic syndrome and obesity, also increases the risk of liver cancer [7].

Long non-coding RNAs (lncRNAs) are a type of RNAs whose transcripts are exceed 200 nt and do not encode proteins [8]. In recent years, with the development of high-throughput technologies, numerous studies have shown that non-coding RNAs are dysregulated in cancer [9]. LncRNAs display multiple biological functions in cancer, including epigenetic regulation, DNA damage and cell cycle regulation, regulation of microRNAs, involvement in signal transduction, mediating proliferation, metastasis, and drug resistance, etc [10–12]. Further, lncRNAs can also influence the development of hepatocellular carcinoma by regulating immune cells. MEG3 can inhibit HCC development by inhibiting M2 macrophage polarization [13]. However, lncRNA-CRNDE can regulates M2 macrophage polarization and promotes angiogenesis in liver cancer [14].

Necroptosis is the programmed cell death with a necrotic appearance [15]. In the process of necroptosis, receptor-binding serine/threonine protein kinase 1/3 (RIPK1/3) and its substrate mixed lineage kinase domain-like protein (MLKL) are key molecules involved in necroptosis. Phosphorylated MLKL translocates to the inner side of the cell membrane and disrupts the integrity of the cell membrane, leading to necroptosis [16]. Cell membrane rupture promotes the release of damage-associated molecular patterns (DAMPs) in the cytoplasm, thereby mediating further inflammatory responses [17,18]. Necroptosis plays an indispensable role in maintaining homeostasis, and is also involved in a series of the pathological processes such as ischemia-reperfusion injury, viral infection, and tumorigenesis [19]. The necroptosis of tumor cells triggers antigenic and inflammatory responses that activate dendritic cells (DCs) and lead to adaptive immunity [20]. A study published in 2017 identified a new apoptosis checkpoint controlled by the molecules RIPK1 and TRAF2 in an experimental mouse model, and found that low expression of RIPK1 and TRAF2 in patients with HCC undergoing resection or liver transplantation was predictive of poor prognosis [21]. However, the latest research shows that RIPK1-RIPK3-MLKL-dependent necroptosis signaling can promote liver cancer in mice by activating NFκb, and drugs targeting the necroptosis response pathway may be a safe and effective strategy to relieve its carcinogenic potential [22].

Numerous studies have demonstrated that lncRNAs play a critical role in a variety of programmed cell death, but few studies have looked at the contribution of necroptosis-related lncRNAs to liver cancer [23]. In this study, systematic bioinformatics analysis was performed to determine the impact of necroptosis-related lncRNAs on the prognosis of the patients with HCC. A risk score prognostic model was developed using differentially expressed necroptosis-related lncRNAs to examine prognosis and tumor microenvironment differences between HCC patients with high-risk and low-risk score, which may provide significant clinical insights regarding the prognosis and response to immunotherapy for patients with HCC.

2. Materials and methods

2.1. Data collection

The RNA-sequence (normal and tumor) transcriptome data and clinical information of HCC patients were downloaded from The Cancer Genome Atlas (TCGA) (https://www.cancer.gov/) database. Samples without survival information were excluded. The single-cell RNA-sequencing data GSE166635 was obtained from the Gene Expression Omnibus (GEO) database. At the same time, the necroptosis-related pathways in Kyoto Encyclopedia of Genes and Genomes (KEGG) database (https://www.genome.jp/dbget-bin/www_bget?pathway+hsa04217) were downloaded, from which a total of 159 necroptosis-related genes (NRGs) were extracted. Using Pearson correlation analysis, the relationship between NRGs and lncRNAs was examined. The criteria for correlation analysis were set to Correlation coefficient >0.4 and $P < 0.001$.

2.2. Differential expression analysis of necroptosis-related lncRNA (NRlncRNAs) and construction of prognostic signature

The *limma* package in R software was used to analyze the differential expression of necroptosis-related lncRNAs (DENRlncRNAs) and filter criteria for screening DENRlncRNAs was set to false discovery rate (FDR) < 0.05 and $|\log_2$ fold change (FC)$|\geq 1.5$. Then the entire TCGA dataset was randomly divided into training and testing groups in a ratio of 7:3. The training group was conducted to construct the necroptosis related lncRNA signature, and then the reliability of the signature was validated through the entire TCGA dataset and testing group. First, to evaluate the correlation between DENRlncRNAs and survival in patients with HCC, a univariate Cox regression analysis was performed using the *survival* package of the R language. In the following steps, LASSO regression analysis was

carried out using the R software package *glmnet*, and the best λ value was taken to determine the optimal risk prediction characteristics, which had a 0.05 *P*-value and tenfold cross-validation. Based on the LASSO analysis results, multivariate regression analysis was performed, and the variables for prognostic models were obtained.

Using the DENRlncRNAs and their coefficients previously determined, each HCC patient's risk score was calculated. The score was determined as:

$$Risk\ score = \sum_{i=1}^{n} Coefi \times xi$$

Coefi is the coefficient and the value of *xi* represents the expression value of each DENRlncRNA selected. Patients with HCC were assigned a risk score based on this formula. According to the median risk score, patients in the training group were divided into high- and low-risk groups. Kaplan-Meier (KM) survival analysis was used to compare the overall survival (OS) rates. Receiver operating characteristic (ROC) curves were established for 1-, 3-, and 5-year OS, from which the areas under the curves (AUCs) could be obtained. PCA (Principal component analysis) analysis and t-SNE (T-distributed stochastic neighbor embedding) analysis were applied for dimensionality reduction. The results were validated using the testing group and the entire dataset.

2.3. Validation of prognostic signatures in clinical characteristics

To examine prognostic signature and clinical characteristics independently, univariate ($P < 0.05$) and multivariate ($P < 0.05$) Cox regression analyses were conducted. Furthermore, a stratified analysis of variables of clinical characteristics was performed, which included stage, gender, grade and T stage. Then KM survival analysis was performed to analyze and compare OS between high-risk and low-risk HCC patients.

2.4. An integrated nomogram based on clinical features and risk score

According to the clinical characteristics of the stage, T stage, age, and risk scores, the nomogram was constructed by Cox regression analysis to evaluate the 1-, 3-, and 5-year survival rate of the HCC patients. The agreement between actual OS and nomogram-predicted OS was assessed by calibration curves. To assess the clinical utility of the nomogram, a decision curve analysis (DCA) and ROC analysis were conducted.

2.5. A network of DENRlncRNAs-NRGs (necroptosis gene), and functional analysis

The Cytoscape was used to investigate co-expression networks of NRGs and lncRNAs in prognostic signatures. Kyoto Encyclopedia of Genes and Genomes (KEGG) and Gene Ontology (GO) analyses of the NRGs in co-expression network were performed using the *clusterProfiler* package [24].

To identify the potential functional pathways involving the necroptosis-related lncRNA signature, Gene Set Enrichment Analysis (GSEA) was conducted [25]. This analysis was carried out with Java GSEA v. 4.0.3 on the KEGG dataset, c2.cp.kegg.v7.5.1.symbols.gmt, to identify enriched pathways between the high- and the low-risk groups. Statistical significance was determined by $|NES| > 1$ and $P < 0.05$.

2.6. Infiltrating immune cells analysis

Immune Cell Infiltration Dataset was downloaded from TIMER2.0 (http://timer.cistrome.org). To evaluate immune cell components or cellular immune responses between high-risk and low-risk groups based on necroptosis-related lncRNA signatures, numerous algorithms were adapted, including xCELL, CIBERSORT, TIMER, QUANTIseq, MCP-counter and EPIC. And a heatmap diagram and correlation dot plot were drawn to show the difference in the infiltrating inmmue cells using different algorithms. Moreover, ssGSEA (Single-sample GSEA) was performed to quantify the subgroup of infiltrating immune cells and estimate their immunity function in both groups. The differential expression of the potential immune checkpionts collected from precious literature was evaluated between the two groups.

2.7. Estimation of tumor microenvironment (TME)

ESTIMATE (Estimation of Stromal and Immune cells in Malignant Tumors using Expression data) is a profiling algorithm for TME, which infers the presence of stromal and immune cells in tumors and determines the purity of tumors by analyzing the expression of specific genes [26,27]. The *Estimate* package in R software was performed to simulate the ratio of the immune and the matrix components in the TME for each sample, presented in the form of three scores: ImmuneScore, StromalScore, and ESTIMATEScore, which were positively correlated with immune, matrix, and the sum of them, respectively. An overall high score is associated with a higher ratio in the TME component corresponding to the score. Moreover, the TME components were compared between groups with high or low risk.

2.8. Assessing the enrichment of NRGs in immune cell subsets using single-cell RNA sequencing data

We downloaded single-cell RNA sequencing data GSE166635 [28] for HCC from the GEO database and performed data quality control and analysis through the *Seurat*, *dplyr*, and *harmony* packages in R software. Samples with feature values greater than 200 and less than 10,000 were selected, and samples with mitochondrial gene percentage greater than 10 were excluded. Data normalization was performed using the NormalizeData function and 2000 genes with high variation coefficients between cells were extracted. Data batch correction was done via the *harmony* package. And PCA and tSNE analysis were performed for data dimensionality reduction and cluster analysis. Cells were divided into multiple distinct subpopulations by combining the *SingleR* package and manual annotation.

Further, the genes in the lncRNA-gene network constructed in section 2.5 were used as the apoptotic gene set, and the AUCell, UCell and singscore algorithms were used to analyze the enrichment of the apoptotic gene set in the immune cell subsets in the single-cell RNA sequencing data. The R packages used in this part of the analysis mainly included *irGSEA*, *Ucell* and *GSEABase*. Finally, GO and KEGG functional analysis were performed on the significantly enriched cell clusters using their top 200 highly variable genes by *clutserProfiler* package [24].

2.9. Quantitative real-time PCR (qRT-PCR) of human liver cancer tissues and cell lines

Three human liver cancer tissue samples and three normal liver tissue samples were obtained from the sample bank of Shuguang Hospital Affiliated to Shanghai University of Traditional Chinese Medicine. PLC-5 and HepG2 are human HCC cell lines, and L02 is the human normal liver cell line. Both lines originated from the Cell Bank of the Chinese Academy of Sciences, China. The human normal liver WRL68 cell line was purchased from Dalian Meilun Biotechnology Co., Ltd (PWE-HU129, meilunbio). In culture, cells were incubated with DMEM (Gibco, USA) supplemented with 10 % FBS (Gibco, USA) and 1 % streptomycin/penicillin (Cellgro, USA). The Total RNA Extraction Reagent (R401, Vazyme, China) was used to isolate total RNA from liver tissue samples and cells. For each sample, the reverse transcription of 1 μg of total RNA to cDNA was performed using HiScript® II Q RT SuperMix for qPCR (+gDNA wiper) (R223, Vazyme, China). ChamQ Universal SYBR qPCR Master Mix (Q711, Vazyme, China) was used for qRT-PCR. The levels of expression of the target lncRNAs were normalized by GAPDH. Table 1 shows the primer sequences used in this study.

2.10. Statistical analysis

In this study, all statistical analyses were performed using R software (version 4.2.1) and its appropriate packages. *P* values less than 0.05 were considered statistically significant. Lasso-Cox regression model was used to determine which DENRlncRNA was significantly correlated with OS, and multivariate COX regression analysis was performed to calculate HR, 95%CI and *P* values to construct a prognostic risk model. In addition, the role of risk scores and other clinical indicators as independent prognostic indicators was also assessed by univariate and multivariate COX regression analyses. Single cell RNA sequencing data were analyzed by *Seurat* package. The independent-samples *t*-test was performed to analyze the quantitative variables.

3. Results

3.1. Data collection and NRlncRNAs identification

The workflow of this study is shown in workflow diagram. After screening for samples with complete survival records and lncRNA expression data downloaded from TCGA database, a total of 371 HCC cases and 50 normal tissue samples were included. Based on 159 necroptosis genes (Supplementary Table 1), a total of 977 NRlncRNAs were obtained, including 425 DENRlncRNAs. A heatmap (Fig. 1A) of the top 50 DENRlncRNAs was built based on these data.

3.2. Construction of the NRlncRNA signature

Randomly, 371 samples were assigned to training and testing groups in a ratio of seven to three. The training group consisted of 260 participants, while the testing group consisted of 111 participants. Using univariate Cox regression to analyze these 425 DENRlncRNAs to screen the NRlncRNA associated with OS in train group, and the results showed that a total of 45 DENRlncRNAs were significantly

Table 1
The primers used for qRT-PCR.

Genes (Human)	Forward primer (5′-3′)	Reverse primer (5′-3′)	Efficiency
PRRT3-AS1	TTCAGAAATGCCTTGCAGTG	CACCTCTTTGCTCTGCTCCT	99.3 %
AL928654.1	AGAGAACTGACTGCTGGAGTGGAG	GAGTATGGGTCGGCTGGAGGAG	106.4 %
MKLN1-AS	GCACTTACTCGGGAAGCCACTG	CGTCCACCTGATGAGACTTCTGAAG	94.3 %
LUCAT1	GCTCGGATTGCCTTAGACAG	GGGTGAGCTTCTTGTGAGGA	102.2 %
POLH-AS1	GGCAGGTGGATCATTTGAGGTCAG	TGAGATGGAGCGTCACTCTGTCG	105.3 %
AL031985.3	CCCTGTCACACCTATTCAACTTCCC	AGCCCTTGAGCCAAACGAAACC	97.8 %
AC040970.1	AACATCTGCCTTTCCTGGTGACAC	TCTCCACCTCGTATCTCCAAACCC	94.5 %
LINC01224	CTCACTACAGCCTCTGCCTCCTAG	AGACACATATCACCTTGGCGTTGG	94.5 %

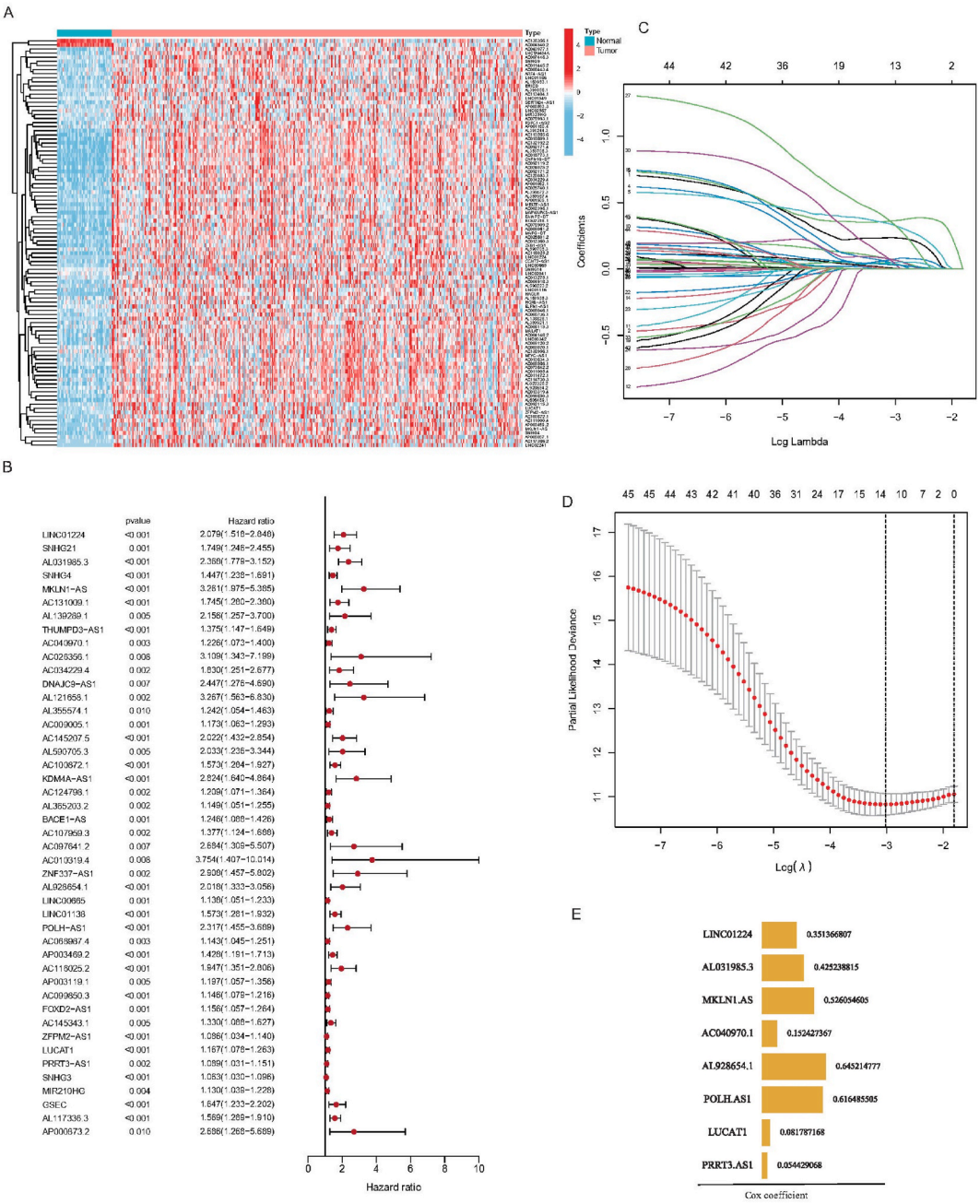

Fig. 1. Construction of a risk score prognostic model based on 8 necroptosis-related lncRNAs. (A) The heatmap of the top 50 DENRlncRNA expression profiles. (B) Univariate analysis of the DENRlncRNAs in HCC. (C, D) LASSO regression analysis. The 45 prognosis-related lncRNAs obtained by Univariate regression analysis were further analyzed by LASSO regression. The coefficient profile is generated by comparing with the log (λ) sequence. Eight predictors of non-zero coefficients were obtained after selecting the optimal λ value (also known as the minimum λ value). (E) Multivariate Cox regression analysis identified 8 necroptosis-related lncRNAs and corresponding coefficients.

associated with OS ($P < 0.01$, Fig. 1B). Next, LASSO regression analysis was performed for further selection of the resulting variables. And 13 necroptosis-related lncRNAs were obtained by LASSO regression analysis. Subsequently, multivariate Cox regression analysis was carried out to determine prognostic necroptosis-lncRNAs. Eight DENRlncRNAs associated with necroptosis (LINC01224, AL031985.3, MKLN1-AS, AC040970.1, AL928654.1, POLH-AS1, LUCAT1, PRRT3-AS1) were identified and considered prognostic indicators (Fig. 1C–E). A predictive signature in the training group based on these 8 necroptosis-related lncRNAs was constructed.

3.3. Survival analysis and the validation of prognostic signature

The prognostic signature based on the 8 DENRlncRNAs was used to perform risk assessment on the samples in the training group. As determined by the median score for each of the HCC patients in the training group, a high-risk group and a low-risk group were formed (Fig. 2A). The distribution of survival status of HCC patients is shown in Fig. 2B. KM survival analysis demonstrated that high-risk participants had a significantly lower OS time than low-risk participants (Fig. 2C). The differential expression of 8 DElncRNAs in the training group are shown in Fig. 2D and a high level of expression was observed for all eight DENRlncRNAs in the high-risk group.

Additionally, the performance of the signature has been evaluated using ROC curves for 1-year, 3-year, and 5-year OS, respectively. And the AUCs at these time points were 0.777, 0.768, and 0.707, respectively (Fig. 2E). In addition, the PCA and t-SNE analyses indicated that low-risk and high-risk groups were significantly different (Fig. 2F and G). Prognostic signatures can be used to distinguish high-risk from low-risk groups, according to these results. To verify the accuracy of the prognostic signatures, the testing group and the entire TCGA dataset were used for validation, which also showed the same results as the training set (Supplementary Fig. 1 and Fig.2).

3.4. Independent prognostic analysis of prognostic signature and clinical characteristic variables

The entire TCGA dataset was used to perform independent prognostic analyzes on the clinical characteristic variables. Univariate Cox regression showed that the HR of the riskScore was 1.165 and the 95 % CI was 1.118–1.215 ($P < 0.001$, Fig. 3A). And multivariate Cox regression showed that the HR of the riskScore was 1.160 and the 95 % CI was 1.108–1.214($P < 0.001$, Fig. 3B). The prognostic signature based on 8 DENRlncRNAs was found to be a significant independent prognostic factor for patients with HCC in both

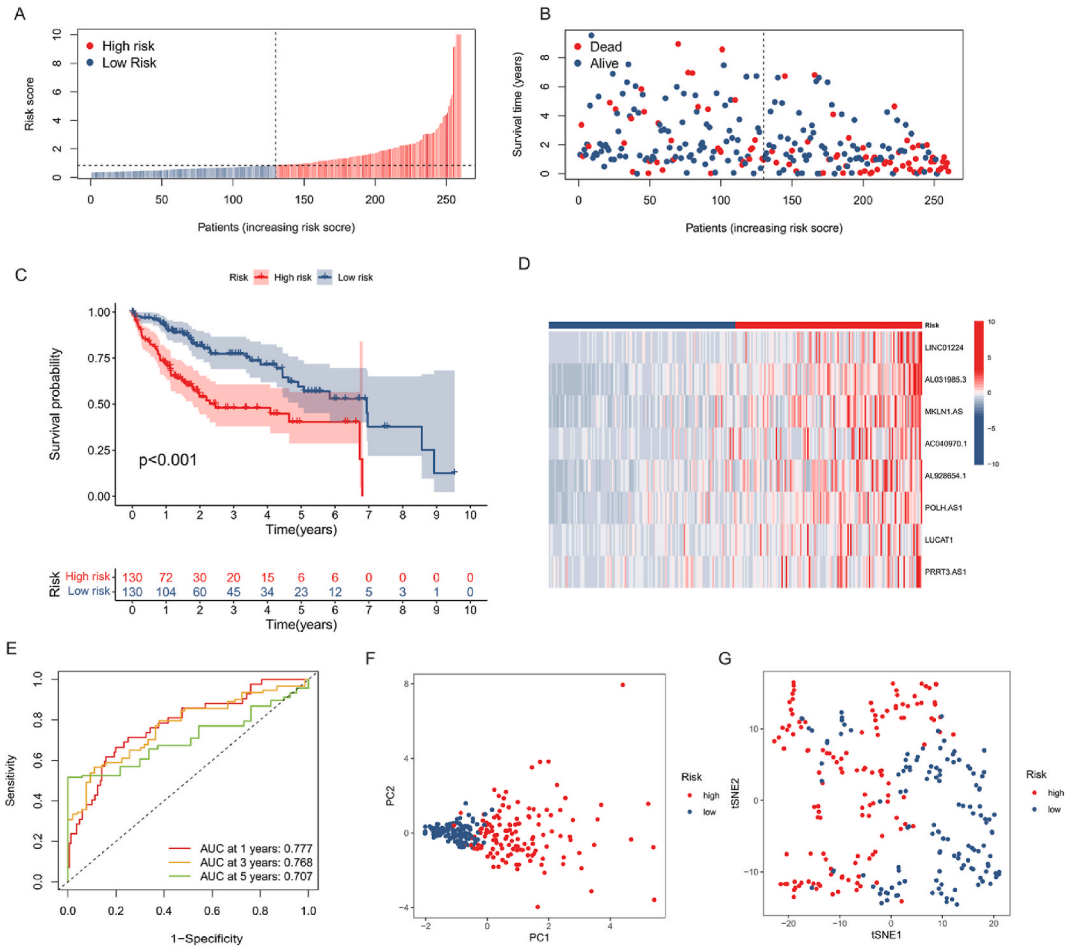

Fig. 2. Risk score prognostic model based on 8 necroptosis-related lncRNAs in the training group. (A, B) Distribution of risk scores and survival status of HCC patients in the training group (The dashed line in the middle represents the median risk score, increasing from left to right). (C) Kaplan–Meier (KM) Survival Analysis of High and Low Risk Groups Grouped by Median Risk Scores in the Training Group. (D) Heatmap showing the expression levels of 8 lncRNAs for each patient in the training group. (E) ROC curves for predicting 1, 3, and 5-year survival of HCC patients in the training group. (F, G) The PCA analysis and tSNE analysis showing the distribution status of high- and low-risk HCC patients in the training group.

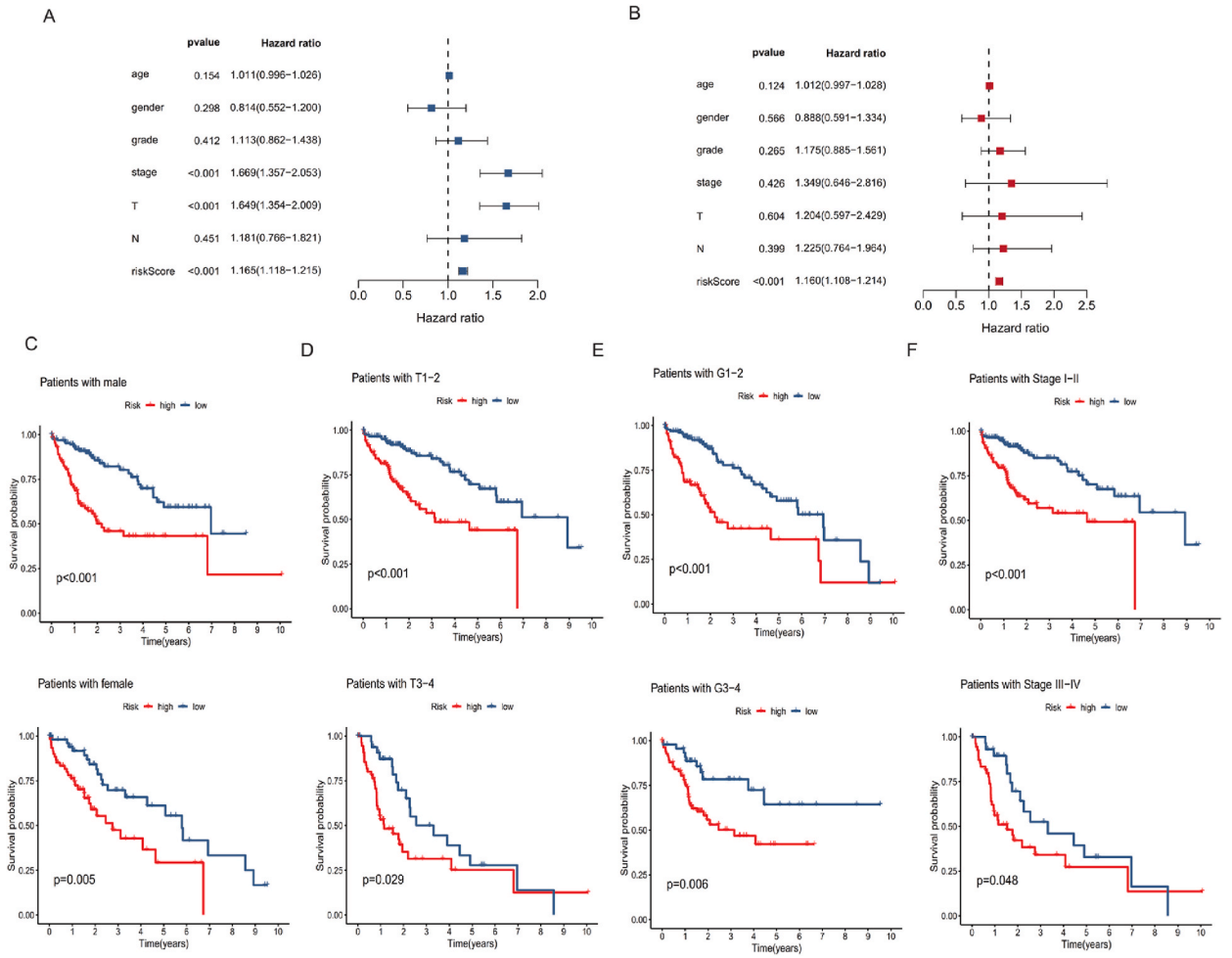

Fig. 3. Independent prognostic analysis of clinical characteristics and risk scores. (A) Univariate regression analysis of clinical characteristics and risk scores. (B) Multivariate regression analysis of clinical characteristics and risk scores. KM analysis of stratified clinical characteristics, including (C) gender, (D) T stage, (E) G stage, (F) stage.

univariate and multivariate regression analyses.

Among the variables of clinical characteristics, univariate analysis showed that stage ($P < 0.001$, HR:1.669, CI:1.357–2.053) and T stage ($P < 0.001$, HR:1.649, CI:1.354–2.009) were independent prognostic factors for patients with HCC.

Survival analysis of stratified clinical variables was performed. The results showed that there was a worse prognosis for high-risk patients than for low-risk patients in different strata of multiple clinical characteristic variables including gender, stage, T stage and grade (Fig. 3C–F).

3.5. Building and validating a nomogram

A nomogram was developed to predict HCC patients' prognosis at different stages of the disease (Fig. 4A). When combined with the scores of various factors in Nomogram, it is possible to predict the survival probability of HCC patients. In the calibration curve, predictions for 1-, 3-, and 5-year survival rates closely matched observations (Fig. 4B and C). Further, the DCA curve demonstrated positive clinical predictive value for HCC patients based on the Nomogram (Fig. 4D).

3.6. DENRlncRNAs-NRGs network map and functional analysis

The GSEA analysis results of the high- and low-risk groups showed that 16 pathways were enriched in the high-risk group, mainly including cell cycle, homologous recombination, spliceosome, ubiquitin mediated proteolysis, DNA replication and so on. In the low-risk group, 12 pathways were enriched, which was mainly involving in substance metabolism, including complement and coagulation cascades, primary bile acid biosynthesis, tryptophan metabolism, fatty acid metabolism, valine leucine and isoleucine degradation, retinol metabolism and so on (Fig. 4E).

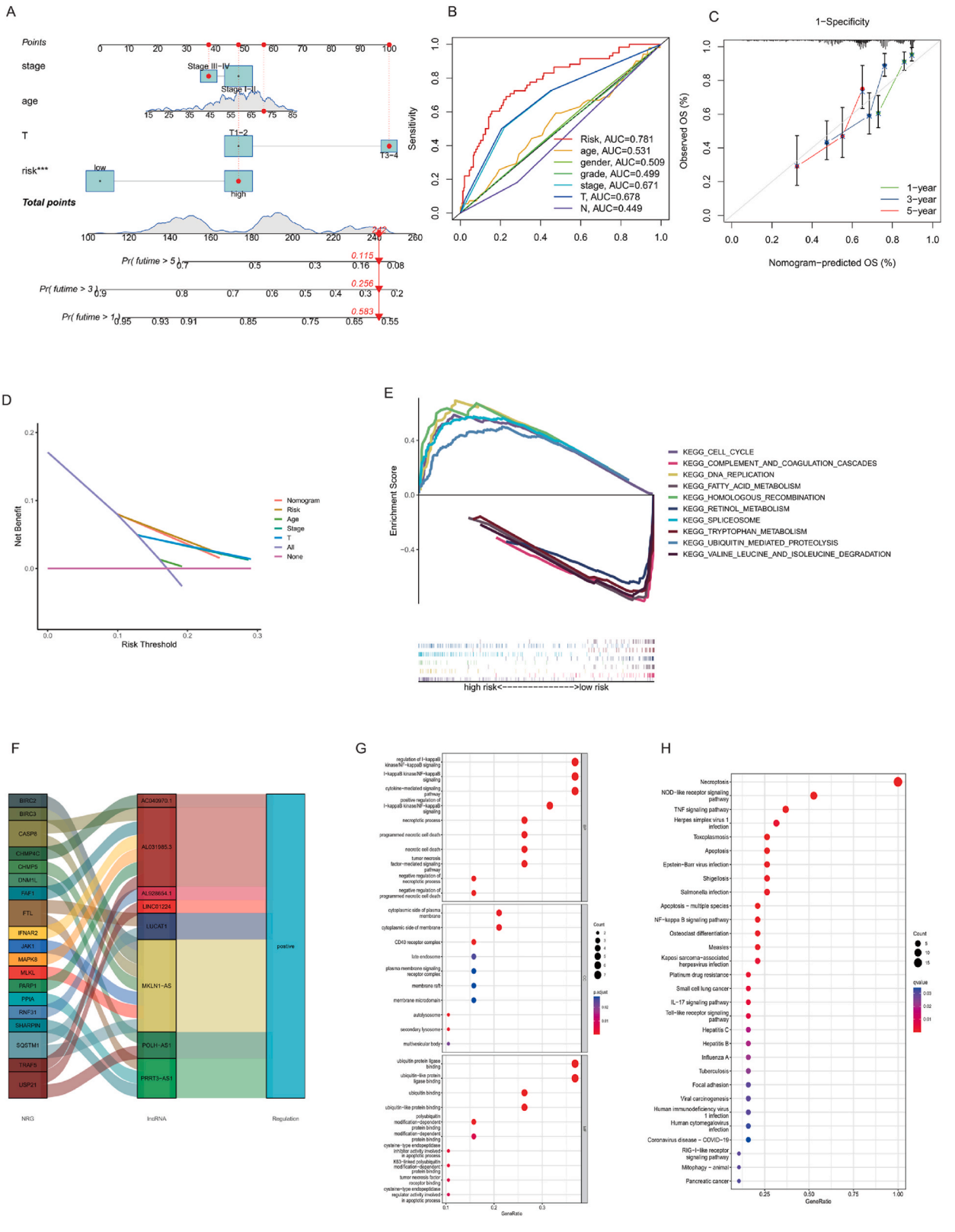

(caption on next page)

Fig. 4. Nomogram of clinical characteristics and risk scores. (A) Nomogram (B) Using ROC curve to show the AUC value of risk score and clinical characteristics predicting 1-year survival in HCC patients. (C, D) The calibration curve and DCA curve demonstrated positive clinical predictive value for HCC patients based on the Nomogram. (E) GSEA analysis for necroptosis-related lncRNAs based on TCGA entire setentire (The pathway above the horizontal axis was active in the high-risk group, and the pathway below the horizontal axis was inhibited in the high-risk group). (F) The co-expression network of 8 necroptosis-related lncRNAs and 19 necroptosis-related genes (The correlation between genes and lncrnas can be obtained by the lines in the figure). (G, H) The GO and KEGG analysis of 19 necroptosis-related genes.

A network was constructed to show the relationship between 8 DENRlncRNAs and NRGs. The results showed that 8 DENRlncRNAs were associated with 19 NRGs (Fig. 4F). According to co-expression analysis of genes and lncRNAs, AL031985.3 has a co-expression relationship with TRAF5, CASP8, MAPK8, FAF1, IFNAR2 and PARP1. POLH-AS1 has a co-expression relationship with DNM1L and USP21. AC040970.1 has a co-expression relationship with CHMP4C. AL928654.1 has a co-expression relationship with RNF31. GO and KEGG enrichment analysis on these 19 NRGs were performed and finally 178 biological processes (BP), 24 molecular functions (MF), 11 cellular components (CC) and 34 pathways ($P < 0.05$, Supplementary Table 2 and Table 3) were obtained. Through the GO biological function and KEGG pathway enrichment analysis of these co-expressed genes, the results showed that the main pathways involved in these genes are not only the necroptosis pathway, but also the IL-17 signaling pathway, Th1 and Th2 cell differentiation, virus infection, and other immune-related pathways. Dot charts were drawn to show the top 10 items of BP, CC, MF in GO analysis (Fig. 4G) and the top 30 pathways of KEGG pathway analysis (Fig. 4H), respectively.

3.7. Immune infiltration analysis and estimation of tumor microenvironment (TME)

The correlation between risk scores and tumor-infiltrating immune cells was examined using several algorithms (Fig. 5A), and the results indicated that infiltrating immune components were strongly associated with risk scores (Fig. 5B), including T cell $CD4^+$ Th2 (Cor = 0.482, $P < 0.001$), Macrophage (Cor = 0.416, $P < 0.001$), Monocyte (Cor = 0.366, $P < 0.001$), Endothelial cell (Cor = −0.555, $P < 0.001$), stroma score (Cor = −0.535, $P < 0.001$) and so on. The heatmap and correlation dot chart of the relationship between high- and low-risk groups and infiltrating immune components is shown in Fig. 5.

Patients at high risk had a low level of immune cell infiltration as determined by immune cell infiltration analysis. An analysis of differential expression of immune checkpoints revealed that the expression levels of multiple immune checkpoints were significantly higher in the high-risk group than in the low-risk group ($P < 0.05$, Fig. 6A). TME analysis of different risk groups revealed significantly lower StromalScores ($P < 0.001$) and EstimateScores ($P < 0.01$) in high-risk groups compared to low-risk groups, although the immune score did not differ significantly ($P > 0.05$, Fig. 6D–F).

Immune cell (Fig. 6B) and related functions (Fig. 6C) based on ssGSEA revealed that there were significant differences in immune cell (activated dendritic cells (aDCs), NK cells, pDCs, Treg) and related function molecules (MHC class I, cytolytic activity, type I, and type II IFN) between high- and low-risk groups.

3.8. Enrichment of necroptosis-related gene sets in immune cell subsets in single-cell RNA sequencing data

A total of 2 single-cell RNA sequencing data samples were obtained for HCC in GSE166635 from the GEO database, and after data quality control (Supplementary Fig. 3-Fig.6), the top 2000 highly variable genes were used for subsequent PCA analysis (Fig. 7A). According to Elbow plot (Fig. 7B), the first 17 principal components (PC) were selected for tSNE cluster analysis. As a result, the cells were divided into 13 clusters (Fig. 7C and D). Though using the *SingleR* package and manual review, finally the cells were divided into 8 types, namely macrophages, monocytes, hepatocytes, Th2 cells, T cells, myofibroblasts, B cells and endothelial cells (Fig. 7E). Then the 19 genes in the lncRNA-gene network were used as a gene set to evaluate the enrichment of the gene set among various cell clusters. According to the results, 19 NRGs were primarily enriched in macrophages, hepatocytes, and monocytes (Fig. 7F). And the results of functional analysis of monocyte clusters (Fig. 7G– H) and macrophage clusters (Fig. 7I– J) with higher enrichment scores showed that the functions involved were mainly in the regulation of T cell activation, antigen processing and presentation, and cell adhesion (Supplementary Table 4 – Table 7).

3.9. Expression of necroptosis gene-related lncRNAs in human liver cancer tissue cell lines

The expression levels of these 8 lncRNAs (LINC01224, AL031985.3, MKLN1-AS, AC040970.1, AL928654.1, POLH-AS1, LUCAT1, PRRT3-AS1) in liver cancer tissues were higher than those in normal liver tissues, and 3 of them (LINC01224, AL928654.1 and MKLN1-AS) had statistically significant differences ($P < 0.05$, Fig. 8A- Fig. 8G).

Besides, the results of the expression levels of eight lncRNAs in human normal liver cell lines (L02, WRL68) and human HCC cell lines (PLC-5, HepG2) showed that, the expression levels of LUCAT1, POLH-AS1 and AL928654.1 in HepG2 and PLC-5 lines were significantly higher than that in L02 cell lines (Fig. 9A). The expression levels of POLH-AS1 and LINC01224 in HepG2 and PLC-5 lines were significantly higher than that in WRL68 cell lines (Fig. 9B).

4. Discussion

Globally, liver cancer ranks fourth in cancer-related deaths and sixth in incidence [29]. The diagnosis of liver cancer mainly relies

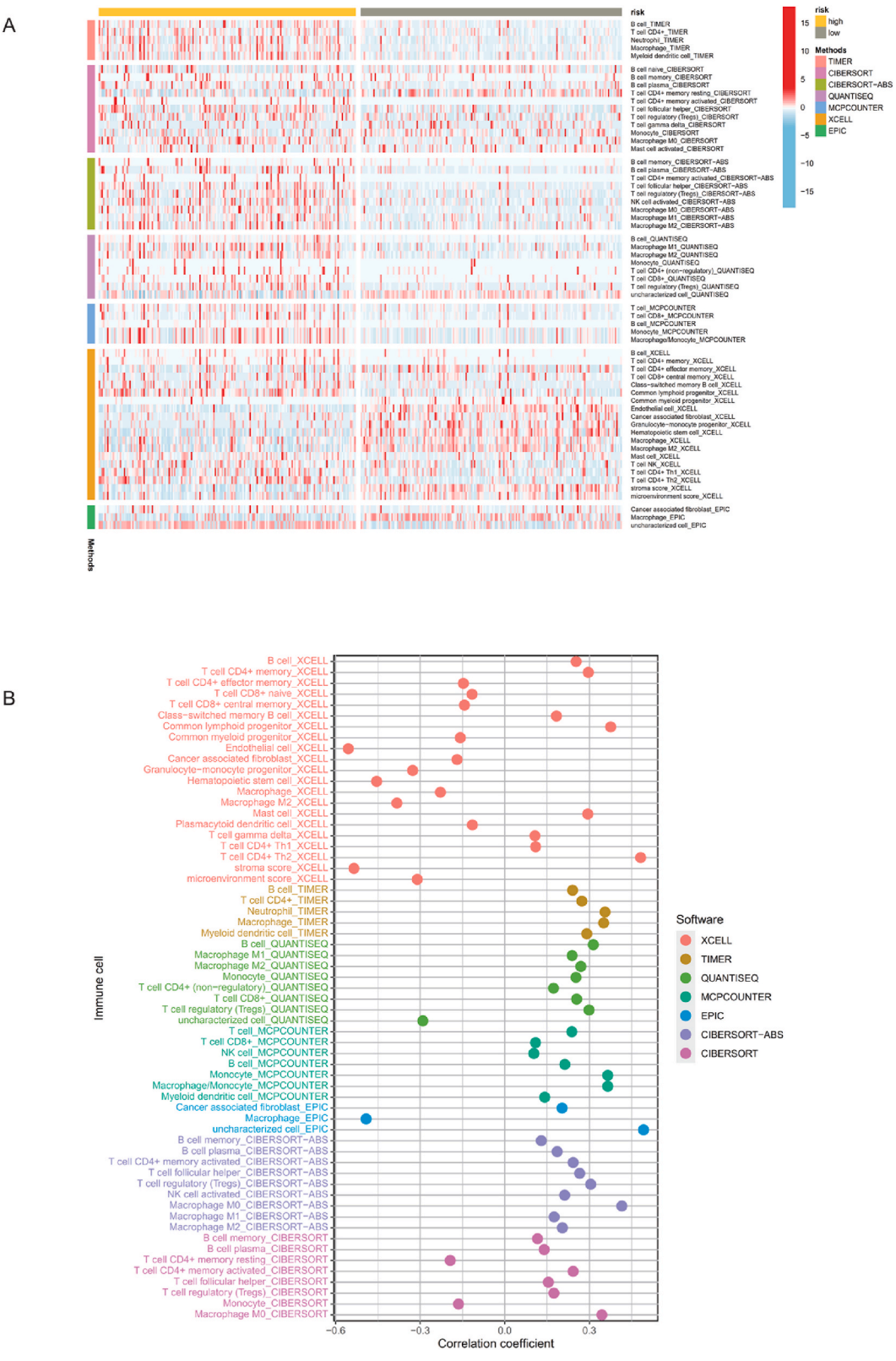

Fig. 5. Heatmap (A) and correlation dot plot (B) for immune infiltration based on TIMER, xCELL, quanTIseq, MCP-counter, CIBERSORT and EPIC algorithms among high- and low-risk groups.

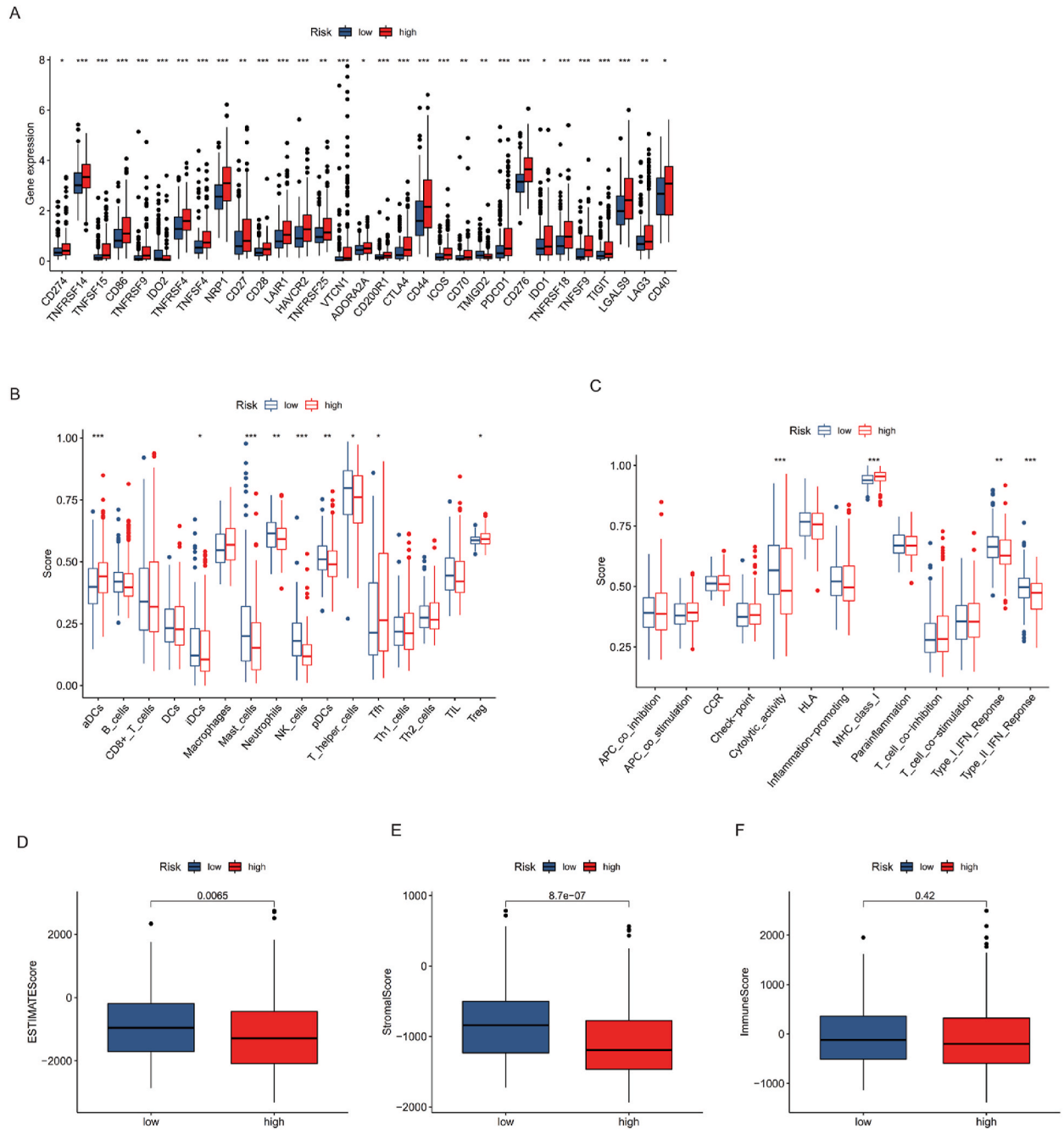

Fig. 6. Analysis of tumor-infiltrating microenvironment. (A) Expression levels of immune checkpoints between high- and low-risk groups. (B, C) ssGSEA for the association between immune cell subpopulations and related functions. The ESTIMATE analysis of (D) ESTIMATEScore, (E) StromalScore, (F)ImmuneScore. (The lower the ESTIMATES score, the more obvious the immunosuppressive effect, $*P < 0.05$, $**P < 0.01$, $***P < 0.001$).

on imaging, serum markers and pathological biopsy. Currently, liver cancer is treated primarily through surgery, hepatic arterial chemoembolization, radiofrequency ablation, molecular targeted therapy, and immunotherapy [30]. Although comprehensive therapeutic strategies have made great progress in the treatment of HCC, the molecular complexity and heterogeneity of HCC make the current therapeutic effects of HCC unsatisfactory [31,32].

A growing body of research evidence shows that there are significant differences in the clinical characteristics and prognosis of HCC patients with different molecular subtypes [33–35]. Necroptosis, a caspase-independent programmed cell death, plays an important role in liver cancer [36]. The necroptosis process, on the other hand, inhibits tumor development by killing tumor cells [21]. However,

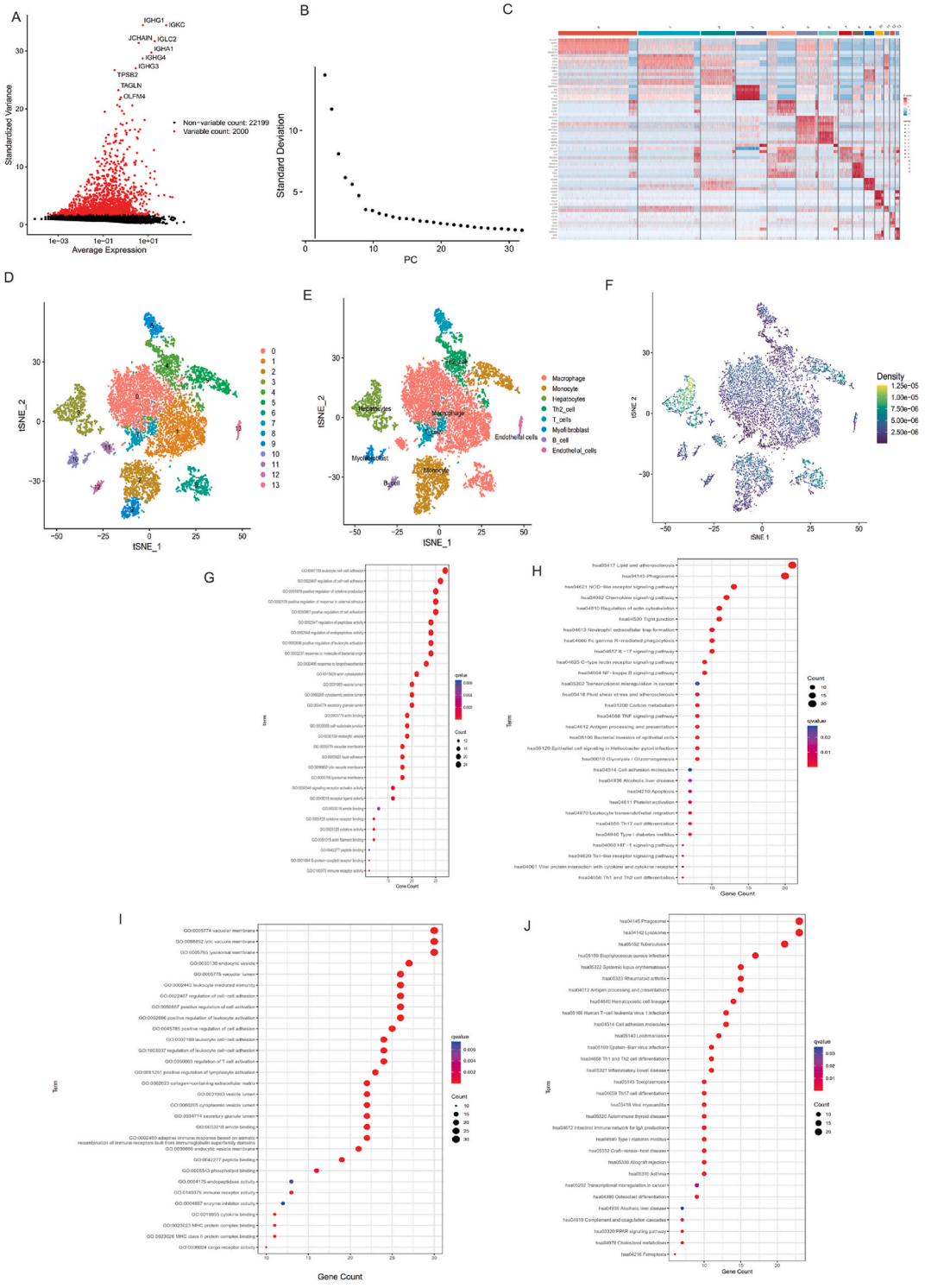

Fig. 7. Single-cell RNA sequencing data analysis of HCC. (A) high variation coefficients between cells. (B) Elbow plot of the PC. (C) Heatmap of the cell clusters. (D) tSNE analysis divides cells into 13 clusters. (E) Cell types of different clusters. (F) Enrichment of necroptosis-related genes in cell clusters. GO and KEGG enrichment analysis of the top 200 highly variable genes in monocyte cluster (G–H) and macrophages cluster (I–J).

necroptosis suppresses the immune system, and the cytokines that are released by necrotic cells promote inflammation that leads to the growth of tumors [37]. With increasing research on necroptosis, targeting necroptosis may become a new strategy for the treatment of HCC [38,39].

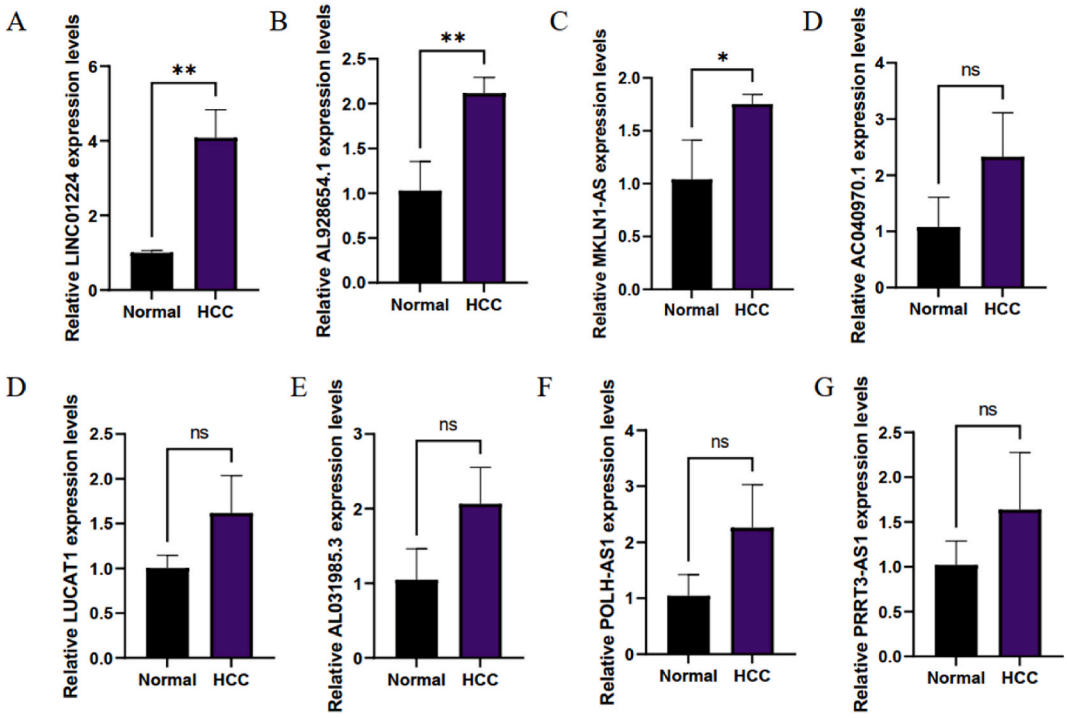

Fig. 8. Expression levels of 8 lncRNAs in human liver cancer tissue and normal liver tissue (Fig.8A–G show the relative expression levels of LINC01224, AL928654.1, MKLN1-AS, AC040970.1, LUCAT1, AL031985.3, POLH-AS1, PRRT3-AS1, respectively; ns, no significance; *, $P < 0.05$; **, $P < 0.01$).

In our analysis of necroptosis-related lncRNAs in HCC patients, we found that they significantly impacted the prognosis of patients with HCC. The study investigated 159 NRGs and identified eight necroptosis-related lncRNAs (including LINC01224, AL031985.3, MKLN1-AS, AC040970.1, AL928654.1, POLH-AS1, LUCAT1, PRRT3-AS1) to develop a prognostic model. We found that patients with HCC have poor prognoses based on the high expression of these 8 lncRNAs in our analysis. Through RT-PCR experiments, we also confirmed that the expression of these 8 lncRNAs was significantly increased in liver cancer tissue. Studies have shown that overexpression of MKLN1-AS can promote the proliferation and epithelial-mesenchymal transition (EMT) of HCC [40], and knockdown of MKLN1-AS significantly inhibits the metastasis and growth of HCC cells in vitro and in vivo. Furthermore, knockdown of MKLN1-AS enhanced the pro-apoptotic effect of lenvatinib [41]. LUCAT1 inhibits the phosphorylation of annexin A2 (ANXA2) and promotes the secretion of plasmin, leading to the activation of metalloproteinase proteins [42]. Upregulation of LUCAT1 expression promotes the development and metastasis of HCC. In addition, the stroma scores for the high-risk group were significantly lower than those for the low-risk group based on the TME analyses on the TCGA dataset. The effect on stromal components in the TME may be one of the mechanisms by which necroptosis-related lncRNAs participate in the incidence and development of HCC. There is evidence that lncRNAs including LINC01224, PRRT3-AS1, AL031985.3 and POLH-AS1 are up-regulated in HCC [43,44], but the specific mechanism is unclear. Furthermore, various studies have demonstrated that these lncRNAs regulate specific microRNAs and promote tumor proliferation and metastasis in the gastrointestinal tract [45,46].

Immunotherapy is one of the effective means of treating cancer. Further studies on the TME will help to develop new and more effective tumor immunotherapy strategies. In this study, there was a strong positive correlation between the risk score and macrophages, neutrophils, and Th2 cells, whereas a negative correlation was identified with endothelial cells and stroma. Overall, our prognostic model indicates poor levels of immune infiltration in patients at high risk. When combined with single-cell sequencing data, necroptosis-related lncRNAs are associated with macrophages in a significant way. There is potential for an exciting new perspective on the immune regulation of lncRNAs that are related to necroptosis in liver cancer due to this finding.

Several types of macrophages inhabit the liver, including yolk sac-derived resident macrophages (Kupffer cells) and peripheral blood mononuclear cells-derived infiltrating macrophages [47]. By utilizing innate immunity, macrophages destroy and eliminate diseased cells. However, macrophages are highly plastic and can be rapidly transformed into tumor-associated macrophages (TAMs) under the influence of the TME. TAMs usually exhibit different functional phenotypes, which are mainly divided into M1-like TAMs and M2-like TAMs. Current studies mainly believe that M1-like TAMs have pro-inflammatory and anti-tumor activities, while M2-like TAMs have anti-inflammatory, immune-suppressing, and tumor-promoting effects [48–50]. Promoting TAM polarization to M1 can activate $CD8^+$ T cell immune responses to suppress HCC [51]. The polarization of TAM to M2 can induce the imbalance of TGF-β1/BMP-7 pathway and promote HCC progression. In addition, M2 macrophages can alter miR-149-5p, which in turn increases the expression of MMP9 in HCC cells, thereby promoting HCC invasion and metastasis [52]. Until now, a few studies have investigated

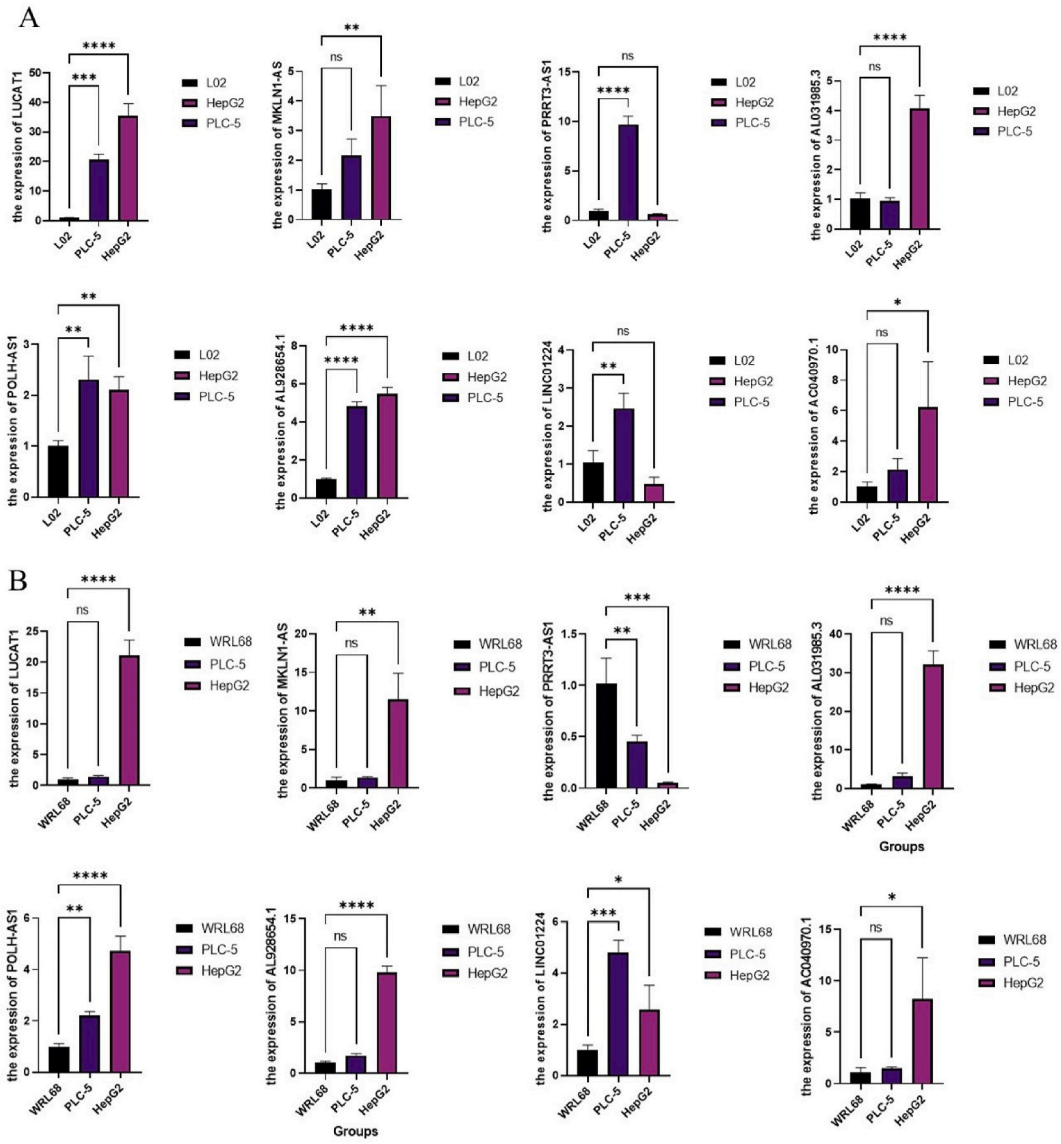

Fig. 9. Expression of eight lncRNAs in different liver cell lines (ns, no significance; *, $P < 0.05$; **, $P < 0.01$; ***, $P < 0.001$; ****, $P < 0.0001$). (A) L02, PLC-5 and HepG2 cell lines; (B) WRL68, PLC-5 and HepG2 cell lines.

the effects of necroptosis-related lncRNAs on macrophages in liver cancer. However, there is evidence to suggest that a parallel network of necrotic apoptosis-induced CXCL1 and Mincle signals promote macrophage-induced adaptive immunosuppression, thereby promoting pancreatic ductal adenocarcinoma progression [53]. Furthermore, The lncRNA is also involved in the regulation of macrophage polarization in liver cancer [13]. The involvement of necroptosis-related lncRNAs in macrophage polarization may contribute to the immune regulation of liver cancer.

TME is the internal environment of tumor cell occurrence and survival, which includes not only tumor cells themselves, but also surrounding fibroblasts, immune and inflammatory cells, stromal cells, microvessels and biomolecules therein. There are a large number of cytokines and growth factors secreted by tumor cells or stromal cells in the TME that contribute to tumor cell growth, angiogenesis, cell metastasis, and resistance to drugs [54]. Studies have shown that the transduction of YAP/TAZ signaling in the TME contributes to the activation of the liver stroma, which in turn promotes anti-cancer drug penetration into the tumor [55]. The influence of stromal components on cancer cells and TME suggests its potential value in anticancer [56,57].

In conclusion, based on eight necroptosis-related long noncoding RNAs, a novel prognostic signature was developed. Our study shows that the necroptosis-related lncRNA risk prognostic model can be used to predict the OS in patients with HCC and is correlated with the characteristics of immune infiltration. Our systematic study of necroptosis-related lncRNAs will serve as a tried effort to understand the role and value of necroptosis-related lncRNAs in HCC. However, it is important to note that the necroptosis-related

lncRNA prognostic model needs to be validated by more external cohorts to clarify its clinical significance. As well, the role of necroptosis-related lncRNA in liver cancer remains unclear, particularly its regulation of immune cells such as macrophages, which needs to be further explored in vivo and in vitro.

Funding

This work was partly supported by National Natural Science Foundation of China (Nos. 82074155, 81973773, China); Program of Shanghai Academic/Technology Research Leader (No. 20XD1423500, China); Shanghai Key Clinical Specialty Construction Project (No. shslczdzk01201, China); Shanghai Frontier Research Base of Disease and Syndrome Biology of inflammatory cancer transformation (No. 2021KJ03-12, China); Shanghai Collaborative Innovation Center of Industrial Transformation of Hospital TCM Preparation (China).

Data availability statement

The data used in this study were derived from the resources available in the public domain. The gene and lncRNA expression profiles and clinical data of the HCC patients in this study were available from TCGA-LIHC in The Cancer Genome Atlas database (TCGA, https://portal.gdc.cancer.gov/repository). The single-cell RNA sequencing data GSE166635 of the HCC could be acquired from Gene Expression Omnibus database (GEO, https://www.ncbi.nlm.nih.gov/geo/query/acc.cgi?acc=GSE166635). The necroptosis-related genes could be acquired in KEGG database (https://www.genome.jp/dbget-bin/www_bget?pathway+hsa04217).

Ethical approval

This study complied with all ethical regulations. Studies involving human participants were reviewed and approved by the Ethics Committee of Shuguang Hospital Affiliated to Shanghai University of Traditional Chinese Medicine (ethics approval number: 2018-629-58-01). Patients provided written informed consent to participate in this study.

CRediT authorship contribution statement

Rongjie Zhang: Writing – review & editing, Writing – original draft, Visualization, Validation, Supervision, Software, Resources, Project administration, Methodology, Investigation, Funding acquisition, Formal analysis, Data curation, Conceptualization. **Qian Li:** Writing – review & editing, Writing – original draft, Validation, Methodology, Investigation, Data curation, Conceptualization. **Xiaoxiao Yu:** Writing – review & editing, Writing – original draft, Validation. **Yiwen Hou:** Validation. **Liang Yan:** Validation. **Yating Gao:** Writing – original draft, Validation. **Longshan Ji:** Writing – review & editing, Writing – original draft. **Xin Zhang:** Funding acquisition, Conceptualization. **Miao Fang:** Supervision, Resources. **Lingying Huang:** Supervision, Resources, Investigation, Funding acquisition. **Zhuo Yu:** Supervision, Funding acquisition. **Yueqiu Gao:** Supervision, Resources, Funding acquisition, Conceptualization. **Man Li:** Writing – review & editing, Supervision, Investigation, Funding acquisition, Conceptualization.

Declaration of competing interest

The authors declare that they have no known competing financial interests or personal relationships that could have appeared to influence the work reported in this paper.

Acknowledgements

We thank the TCGA and GEO databases as well as KEGG database for the availability of the data.

Abbreviations

LncRNA	Long non-coding RNA
HCC	hepatocellular carcinoma
LASSO	least absolute shrinkage and selection operator algorithm
HBV	hepatitis B virus
NAFLD	nonalcoholic fatty liver disease
MLKL	mixed lineage kinase domain-like protein
DCs	dendritic cells
NRGs	necroptosis-related genes
DENRlncRNAs	differential expression of necroptosis-related lncRNAs
DCA	decision curve analysis
OS	overall survival
AUCs	areas under the curves
ROC	Receiver operating characteristic

TME Tumor Microenvironment
TAMs tumor-associated macrophages

Appendix A. Supplementary data

Supplementary data to this article can be found online at https://doi.org/10.1016/j.heliyon.2023.e22083.

References

[1] W. Chen, R. Zheng, P.D. Baade, S. Zhang, H. Zeng, F. Bray, A. Jemal, X.Q. Yu, J. He, Cancer statistics in China, 2015, CA Cancer J Clin 66 (2) (2016) 115–132.
[2] M. Sayiner, P. Golabi, Z.M. Younossi, Disease burden of hepatocellular carcinoma: a global perspective, Dig. Dis. Sci. 64 (4) (2019) 910–917.
[3] D. Anwanwan, S.K. Singh, S. Singh, V. Saikam, R. Singh, Challenges in liver cancer and possible treatment approaches, Biochim. Biophys. Acta Rev. Canc 1873 (1) (2020), 188314.
[4] M.M. Center, A. Jemal, International trends in liver cancer incidence rates, Cancer Epidemiol. Biomarkers Prev. 20 (11) (2011) 2362–2368.
[5] C. Bosetti, F. Turati, C. La Vecchia, Hepatocellular carcinoma epidemiology, Best Pract. Res. Clin. Gastroenterol. 28 (5) (2014) 753–770.
[6] C. de Martel, D. Maucort-Boulch, M. Plummer, S. Franceschi, World-wide relative contribution of hepatitis B and C viruses in hepatocellular carcinoma, Hepatology 62 (4) (2015) 1190–1200.
[7] Z. Younossi, M. Stepanova, J.P. Ong, I.M. Jacobson, E. Bugianesi, A. Duseja, Y. Eguchi, V.W. Wong, F. Negro, Y. Yilmaz, et al., Nonalcoholic steatohepatitis is the fastest growing cause of hepatocellular carcinoma in liver transplant candidates, Clin. Gastroenterol. Hepatol. 17 (4) (2019) 748–755.e743.
[8] A. Sahu, U. Singhal, A.M. Chinnaiyan, Long noncoding RNAs in cancer: from function to translation, Trends Cancer 1 (2) (2015) 93–109.
[9] Z. Huang, J.K. Zhou, Y. Peng, W. He, C. Huang, The role of long noncoding RNAs in hepatocellular carcinoma, Mol. Cancer 19 (1) (2020) 77.
[10] L. Ma, A. Xu, L. Kang, R. Cong, Z. Fan, X. Zhu, N. Huo, W. Liu, C. Xue, Q. Ji, et al., LSD1-Demethylated LINC01134 confers oxaliplatin resistance through SP1-induced p62 transcription in HCC, Hepatology 74 (6) (2021) 3213–3234.
[11] J. Feng, G. Yang, Y. Liu, Y. Gao, M. Zhao, Y. Bu, H. Yuan, Y. Yuan, H. Yun, M. Sun, et al., LncRNA PCNAP1 modulates hepatitis B virus replication and enhances tumor growth of liver cancer, Theranostics 9 (18) (2019) 5227–5245.
[12] H. Wang, X. Huo, X.R. Yang, J. He, L. Cheng, N. Wang, X. Deng, H. Jin, N. Wang, C. Wang, et al., STAT3-mediated upregulation of lncRNA HOXD-AS1 as a ceRNA facilitates liver cancer metastasis by regulating SOX4, Mol. Cancer 16 (1) (2017) 136.
[13] Q. Wei, G. Liu, Z. Huang, Y. Huang, L. Huang, Z. Huang, X. Wu, H. Wei, J. Pu, LncRNA MEG3 inhibits tumor progression by modulating macrophage phenotypic polarization via miR-145-5p/DAB2 Axis in hepatocellular carcinoma, J. Hepatocell. Carcinoma 10 (2023) 1019–1035.
[14] C. Han, Y. Yang, Y. Sheng, J. Wang, W. Li, X. Zhou, L. Guo, The mechanism of lncRNA-CRNDE in regulating tumour-associated macrophage M2 polarization and promoting tumour angiogenesis, J. Cell Mol. Med. 25 (9) (2021) 4235–4247.
[15] A. Degterev, Z. Huang, M. Boyce, Y. Li, P. Jagtap, N. Mizushima, G.D. Cuny, T.J. Mitchison, M.A. Moskowitz, J. Yuan, Chemical inhibitor of nonapoptotic cell death with therapeutic potential for ischemic brain injury, Nat. Chem. Biol. 1 (2) (2005) 112–119.
[16] Z. Cai, Z.G. Liu, Execution of RIPK3-regulated necrosis, Mol Cell Oncol 1 (2) (2014), e960759.
[17] A. Kaczmarek, P. Vandenabeele, D.V. Krysko, Necroptosis: the release of damage-associated molecular patterns and its physiological relevance, Immunity 38 (2) (2013) 209–223.
[18] L. Zhou, J. Lyu, F. Liu, Y. Su, L. Feng, X. Zhang, Immunogenic PANoptosis-initiated cancer sono-immune reediting nanotherapy by iteratively boosting cancer immunity cycle, Adv Mater (2023), e2305361.
[19] R. Weinlich, A. Oberst, H.M. Beere, D.R. Green, Necroptosis in development, inflammation and disease, Nat. Rev. Mol. Cell Biol. 18 (2) (2017) 127–136.
[20] N. Yatim, H. Jusforgues-Saklani, S. Orozco, O. Schulz, R. Barreira da Silva, C. Reis e Sousa, D.R. Green, A. Oberst, M.L. Albert, RIPK1 and NF-κB signaling in dying cells determines cross-priming of CD8$^+$ T cells, Science 350 (6258) (2015) 328–334.
[21] A.T. Schneider, J. Gautheron, M. Feoktistova, C. Roderburg, S.H. Loosen, S. Roy, F. Benz, P. Schemmer, M.W. Büchler, U. Nachbur, et al., RIPK1 suppresses a TRAF2-dependent pathway to liver cancer, Cancer Cell 31 (1) (2017) 94–109.
[22] M. Vucur, A. Ghallab, A.T. Schneider, A. Adili, M. Cheng, M. Castoldi, M.T. Singer, V. Büttner, L.S. Keysberg, L. Küsgens, et al., Sublethal necroptosis signaling promotes inflammation and liver cancer, Immunity 56 (7) (2023) 1578–1595.e1578.
[23] N. Jiang, X. Zhang, X. Gu, X. Li, L. Shang, Progress in understanding the role of lncRNA in programmed cell death, Cell Death Discov 7 (1) (2021) 30.
[24] G. Yu, L.G. Wang, Y. Han, Q.Y. He, clusterProfiler: an R package for comparing biological themes among gene clusters, OMICS 16 (5) (2012) 284–287.
[25] A. Subramanian, P. Tamayo, V.K. Mootha, S. Mukherjee, B.L. Ebert, M.A. Gillette, A. Paulovich, S.L. Pomeroy, T.R. Golub, E.S. Lander, et al., Gene set enrichment analysis: a knowledge-based approach for interpreting genome-wide expression profiles, Proc Natl Acad Sci U S A 102 (43) (2005) 15545–15550.
[26] K. Yoshihara, M. Shahmoradgoli, E. Martínez, R. Vegesna, H. Kim, W. Torres-Garcia, V. Treviño, H. Shen, P.W. Laird, D.A. Levine, et al., Inferring tumour purity and stromal and immune cell admixture from expression data, Nat. Commun. 4 (2013) 2612.
[27] H. Qiu, Y. Li, S. Cheng, J. Li, C. He, J. Li, A prognostic microenvironment-related immune signature via ESTIMATE (PROMISE model) predicts overall survival of patients with glioma, Front. Oncol. 10 (2020), 580263.
[28] Y. Meng, Q. Zhao, L. An, S. Jiao, R. Li, Y. Sang, J. Liao, P. Nie, F. Wen, J. Ju, et al., A TNFR2-hnRNPK Axis promotes primary liver cancer development via activation of YAP signaling in hepatic progenitor cells, Cancer Res. 81 (11) (2021) 3036–3050.
[29] A. Villanueva, Hepatocellular carcinoma, N. Engl. J. Med. 380 (15) (2019) 1450–1462.
[30] A. Forner, M. Reig, J. Bruix, Hepatocellular carcinoma, Lancet 391 (10127) (2018) 1301–1314.
[31] C. Fitzmaurice, C. Allen, R.M. Barber, L. Barregard, Z.A. Bhutta, H. Brenner, D.J. Dicker, O. Chimed-Orchir, R. Dandona, L. Dandona, et al., Global, regional, and national cancer incidence, mortality, years of life lost, years lived with disability, and disability-adjusted life-years for 32 cancer groups, 1990 to 2015: a systematic analysis for the global burden of disease study, JAMA Oncol. 3 (4) (2017) 524–548.
[32] J. Zucman-Rossi, A. Villanueva, J.C. Nault, J.M. Llovet, Genetic landscape and biomarkers of hepatocellular carcinoma, Gastroenterology 149 (5) (2015) 1226–1239.e1224.
[33] C. Fang, S. Liu, K. Feng, C. Huang, Y. Zhang, J. Wang, H. Lin, J. Wang, C. Zhong, Ferroptosis-related lncRNA signature predicts the prognosis and immune microenvironment of hepatocellular carcinoma, Sci. Rep. 12 (1) (2022) 6642.
[34] P. Lin, R.Z. Gao, R. Wen, Y. He, H. Yang, DNA damage repair profiles alteration characterize a hepatocellular carcinoma subtype with unique molecular and clinicopathologic features, Front. Immunol. 12 (2021), 715460.
[35] S.M. Ahn, S.J. Jang, J.H. Shim, D. Kim, S.M. Hong, C.O. Sung, D. Baek, F. Haq, A.A. Ansari, S.Y. Lee, et al., Genomic portrait of resectable hepatocellular carcinomas: implications of RB1 and FGF19 aberrations for patient stratification, Hepatology 60 (6) (2014) 1972–1982.
[36] D. Ofengeim, J. Yuan, Regulation of RIP1 kinase signalling at the crossroads of inflammation and cell death, Nat. Rev. Mol. Cell Biol. 14 (11) (2013) 727–736.
[37] B. Strilic, L. Yang, J. Albarrán-Juárez, L. Wachsmuth, K. Han, U.C. Müller, M. Pasparakis, S. Offermanns, Tumour-cell-induced endothelial cell necroptosis via death receptor 6 promotes metastasis, Nature 536 (7615) (2016) 215–218.
[38] M. Vucur, F. Reisinger, J. Gautheron, J. Janssen, C. Roderburg, D.V. Cardenas, K. Kreggenwinkel, C. Koppe, L. Hammerich, R. Hakem, et al., RIP3 inhibits inflammatory hepatocarcinogenesis but promotes cholestasis by controlling caspase-8- and JNK-dependent compensatory cell proliferation, Cell Rep. 4 (4) (2013) 776–790.

[39] Q. Zeng, X. Ma, Y. Song, Q. Chen, Q. Jiao, L. Zhou, Targeting regulated cell death in tumor nanomedicines, Theranostics 12 (2) (2022) 817–841.
[40] C. Guo, S. Zhou, W. Yi, P. Yang, O. Li, J. Liu, C. Peng, SOX9/MKLN1-AS Axis induces hepatocellular carcinoma proliferation and epithelial-mesenchymal transition, Biochem. Genet. 60 (6) (2022) 1914–1933.
[41] X. Chen, Q. Ye, Z. Chen, Q. Lin, W. Chen, C. Xie, X. Wang, Long non-coding RNA muskelin 1 antisense RNA as a potential therapeutic target in hepatocellular carcinoma treatment, Bioengineered 13 (5) (2022) 12237–12247.
[42] Y. Lou, Y. Yu, X. Xu, S. Zhou, H. Shen, T. Fan, D. Wu, J. Yin, G. Li, Long non-coding RNA LUCAT1 promotes tumourigenesis by inhibiting ANXA2 phosphorylation in hepatocellular carcinoma, J. Cell Mol. Med. 23 (3) (2019) 1873–1884.
[43] P. Zhou, Y. Lu, Y. Zhang, L. Wang, Construction of an immune-related six-lncRNA signature to predict the outcomes, immune cell infiltration, and immunotherapy response in patients with hepatocellular carcinoma, Front. Oncol. 11 (2021), 661758.
[44] Z. Zhang, W. Zhang, Y. Wang, T. Wan, B. Hu, C. Li, X. Ge, S. Lu, Construction and validation of a ferroptosis-related lncRNA signature as a novel biomarker for prognosis, immunotherapy and targeted therapy in hepatocellular carcinoma, Front. Cell Dev. Biol. 10 (2022), 792676.
[45] J. Gu, L. Dong, Y. Wang, W. Nie, W. Liu, J.A. Zhao, LINC01224 promotes colorectal cancer progression through targeting miR-485-5p/MYO6 axis, World J. Surg. Oncol. 19 (1) (2021) 281.
[46] H. Sun, J. Yan, G. Tian, X. Chen, W. Song, LINC01224 accelerates malignant transformation via MiR-193a-5p/CDK8 axis in gastric cancer, Cancer Med. 10 (4) (2021) 1377–1393.
[47] Z. Bian, Y. Gong, T. Huang, C.Z.W. Lee, L. Bian, Z. Bai, H. Shi, Y. Zeng, C. Liu, J. He, et al., Deciphering human macrophage development at single-cell resolution, Nature 582 (7813) (2020) 571–576.
[48] Y.L. Zhang, Q. Li, X.M. Yang, F. Fang, J. Li, Y.H. Wang, Q. Yang, L. Zhu, H.Z. Nie, X.L. Zhang, et al., SPON2 promotes M1-like macrophage recruitment and inhibits hepatocellular carcinoma metastasis by distinct integrin-rho GTPase-hippo pathways, Cancer Res. 78 (9) (2018) 2305–2317.
[49] Y. Ye, Y. Xu, Y. Lai, W. He, Y. Li, R. Wang, X. Luo, R. Chen, T. Chen, Long non-coding RNA cox-2 prevents immune evasion and metastasis of hepatocellular carcinoma by altering M1/M2 macrophage polarization, J. Cell. Biochem. 119 (3) (2018) 2951–2963.
[50] C.Y. Wei, M.X. Zhu, P.F. Zhang, X.Y. Huang, J.K. Wan, X.Z. Yao, Z.T. Hu, X.Q. Chai, R. Peng, X. Yang, et al., PKCα/ZFP64/CSF1 axis resets the tumor microenvironment and fuels anti-PD1 resistance in hepatocellular carcinoma, J. Hepatol. 77 (1) (2022) 163–176.
[51] J. Ning, Y. Ye, D. Bu, G. Zhao, T. Song, P. Liu, W. Yu, H. Wang, H. Li, X. Ren, et al., Imbalance of TGF-β1/BMP-7 pathways induced by M2-polarized macrophages promotes hepatocellular carcinoma aggressiveness, Mol. Ther. 29 (6) (2021) 2067–2087.
[52] G. Liu, L. Yin, X. Ouyang, K. Zeng, Y. Xiao, Y. Li, M2 macrophages promote HCC cells invasion and migration via miR-149-5p/MMP9 signaling, J. Cancer 11 (5) (2020) 1277–1287.
[53] L. Seifert, G. Werba, S. Tiwari, N.N. Giao Ly, S. Alothman, D. Alqunaibit, A. Avanzi, R. Barilla, D. Daley, S.H. Greco, et al., The necrosome promotes pancreatic oncogenesis via CXCL1 and Mincle-induced immune suppression, Nature 532 (7598) (2016) 245–249.
[54] T. Wu, Y. Dai, Tumor microenvironment and therapeutic response, Cancer Lett. 387 (2017) 61–68.
[55] K. Cho, S.W. Ro, H.W. Lee, H. Moon, S. Han, H.R. Kim, S.H. Ahn, J.Y. Park, D.Y. Kim, YAP/TAZ suppress drug penetration into hepatocellular carcinoma through stromal activation, Hepatology 74 (5) (2021) 2605–2621.
[56] J. Liu, P. Li, L. Wang, M. Li, Z. Ge, L. Noordam, R. Lieshout, M.M.A. Verstegen, B. Ma, J. Su, et al., Cancer-associated fibroblasts provide a stromal niche for liver cancer organoids that confers trophic effects and therapy resistance, Cell Mol Gastroenterol Hepatol 11 (2) (2021) 407–431.
[57] F. Yang, Y. Wei, D. Han, Y. Li, S. Shi, D. Jiao, J. Wu, Q. Zhang, C. Shi, L. Yang, et al., Interaction with CD68 and regulation of GAS6 expression by endosialin in fibroblasts drives recruitment and polarization of macrophages in hepatocellular carcinoma, Cancer Res. 80 (18) (2020) 3892–3905.